

<b>Project acronym:</b>	<b>Geo-Drill</b>		
<b>Project title:</b>	Development of novel and Cost-Effective drilling technology for geothermal Systems		
<b>Activity:</b>	LCE-07-17-Renewables		
<b>Call:</b>	H2020-LC-SC3-2018-RES-TwoStages		
<b>Funding Scheme:</b>	RIA	<b>Grant Agreement</b>	815319
<b>WP 3</b>	<b>Material Testing and Characterization</b>		

### D3.6 – Impact of welding on coating integrity

<b>Due date:</b>	31/05/2021 (M25)		
<b>Actual Submission Date:</b>	23/11/2021		
<b>Lead Beneficiary:</b>	TWI		
<b>Main authors/contributors:</b>	TWI		
<b>Dissemination Level<sup>1</sup>:</b>	PU		
<b>Nature:</b>	REPORT		
<b>Status of this version:</b>		<b>Draft under Development</b>	
		<b>For Review by Coordinator</b>	
	X	<b>Submitted</b>	
<b>Version:</b>	1.0		
<b>Abstract</b>	The deliverable reports on the Welding processes were reviewed in the context of the materials and geometry of the drill pipe components.		

#### REVISION HISTORY

Version	Date	Main Authors/Contributors	Description of changes

<sup>1</sup> Dissemination level security:

**PU** – Public (e.g. on website, for publication etc.) / **PP** – Restricted to other programme participants (incl. Commission services) /

**RE** – Restricted to a group specified by the consortium (incl. Commission services) / **CO** – confidential, only for members of the consortium (incl. Commission services)



This project has received funding from the *European Union's Horizon 2020 research and innovation programme* under grant agreement No 815319



*This project has received funding from the European Union's Horizon 2020 program Grant Agreement No 815319. This publication reflects the views only of the author(s), and the Commission cannot be held responsible for any use which may be made of the information contained therein.*

**Copyright © 2019-2023, Geo-Drill Consortium**

This document and its contents remain the property of the beneficiaries of the Geo-Drill Consortium and may not be distributed or reproduced without the express written approval of the Geo-Drill Coordinator, TWI Ltd. ([www.twi-global.com](http://www.twi-global.com))

*THIS DOCUMENT IS PROVIDED BY THE COPYRIGHT HOLDERS AND CONTRIBUTORS "AS IS" AND ANY EXPRESS OR IMPLIED WARRANTIES, INCLUDING, BUT NOT LIMITED TO, THE IMPLIED WARRANTIES OF MERCHANTABILITY AND FITNESS FOR A PARTICULAR PURPOSE ARE DISCLAIMED. IN NO EVENT SHALL THE COPYRIGHT OWNER OR CONTRIBUTORS BE LIABLE FOR ANY DIRECT, INDIRECT, INCIDENTAL, SPECIAL, EXEMPLARY, OR CONSEQUENTIAL DAMAGES (INCLUDING, BUT NOT LIMITED TO, PROCUREMENT OF SUBSTITUTE GOODS OR SERVICES; LOSS OF USE, DATA, OR PROFITS; OR BUSINESS INTERRUPTION) HOWEVER CAUSED AND ON ANY THEORY OF LIABILITY, WHETHER IN CONTRACT, STRICT LIABILITY, OR TORT (INCLUDING NEGLIGENCE OR OTHERWISE) ARISING IN ANY WAY OUT OF THE USE OF THIS DOCUMENT, EVEN IF ADVISED OF THE POSSIBILITY OF SUCH DAMAGE.*

### **Objectives of task T3.6**

- TWI will review the welding processes available based on the materials and geometry of the components to be welded. ✓
- Based on the initial review TWI will select the most appropriate process and produce test coupons. ✓
- Perform welding test on coupons: Selection of test points and optimization of parameters will be supported by adaptive DoE and meta-modelling. ✓
- The welding parameters will be optimized to achieve a uniform, defect-free weld. ✓
- The consumables will be selected based on their availability and corrosion performance.

### **Summary of work**

The following work was undertaken to meet the above objectives and is described in this report, D3.6

- Welding processes were reviewed in the context of the materials and geometry of the drill pipe components.
- Following the review, Rotary Friction welding was selected as the most suitable process.
- Rotary friction welding was used to produce test coupons, parameters were selected to form a Design of Experiments (DoE) matrix.
- All the welding parameters selected achieved a uniform, defect-free weld.
- DoE software was employed to optimise parameter selection in relation to peak hardness and ultimate tensile strength.
- Weld coupons were made using optimised parameters for testing of a WC-CoCr coating (36WC) and a self-fluxing coating (36Flux) coating.
- The rotary friction welding process does not seem to have an impact on the coating integrity. Both cermet and alloy HVOF sprayed coatings seem to behave similarly close to the weld interface (at the Heat Affected Zone or HAZ) as compared with the parent metals.
  - Consumables are not required for the joining technology selected (rotary friction welding), as such there are no issues relating to their availability or corrosion resistance.
- This Work Package (WP) has increased the consortium's understanding of the effect of welding on coating integrity.

## CONTENTS

OBJECTIVES OF TASK T3.6 .....	4
SUMMARY OF WORK .....	4
1. INTRODUCTION .....	6
1.1 DRILL PIPE JOINING REVIEW .....	6
1.2 ROTARY FRICTION WELDING.....	7
2. EXPERIMENTAL DETAILS.....	9
2.1 ROTARY FRICTION WELDING.....	9
2.1.1 Materials .....	9
2.1.2 Welding Equipment.....	9
2.1.3 Part Preparation.....	10
2.1.4 Welding Trials.....	11
2.1.5 Metallurgical analysis.....	12
2.1.6 Tensile testing .....	12
2.1.7 Design of Experiments .....	13
2.2 COATING DEPOSITION.....	13
2.2.1 Materials .....	13
2.2.2 HVOF spray set-up.....	14
2.3 COATING CHARACTERISATION .....	16
2.3.1 Microstructure characterisation .....	16
2.3.2 Scratch test.....	16
3. RESULTS AND DISCUSSION .....	17
3.1 WELDING TRIALS.....	17
3.1.1 Cross Weld Tensile Testing.....	18
3.1.2 Microstructural assessment.....	18
3.1.3 Design of Experiments .....	20
3.2 COATINGS ON WELDS .....	20
4. CONCLUSIONS .....	30
REFERENCES.....	30
APPENDIX A: PHOTOGRAPHS OF COMPLETE WELDS .....	31
APPENDIX B: PHOTOGRAPHS OF FAILED TENSILE SAMPLES .....	35
APPENDIX C: MACRO-IMAGES OF THE WELD INTERFACE .....	39

## 1. INTRODUCTION

### 1.1 Drill Pipe Joining Review

The geo-drill project aims to enable a cost effective down-the hole (DTH) technology suitable for geothermal drilling. Drill pipes are employed in high torque environments deep within the earth's crust, they must withstand high pressure and torque. As such, drill pipe tends to be manufactured from a carbon or high strength steel. Modern drill pipe is manufactured from separate pieces, most commonly the tool joint and tube body.

The tool joint provides high strength, high pressure connections between drill pipes and therefore tend to be produced with higher strength steel than the tube body. The dissimilar steel sections required welding together to produce a drill pipe. The following section outlines the advantages and disadvantages of potential joining technologies and the reasoning behind the selection of friction welding for this project.

The materials identified for this body of work were AISI 4140 and N80. AISI 410 is a Cr-Mo-Mn-based high strength, low alloy, medium carbon steel. When considering these materials for fusion welding, in particular arc welding there are a number of factors to consider. In arc welding, high local heat input melts the base and filler metals, which results in the formation of the weld pool shape, weld imperfections and defects and critically microstructural changes in the Heat Affected Zone (HAZ) [1].

These changes in the HAZ cause contribute to two key phenomena; firstly post-weld residual stresses and distortion [1] and secondly high levels of hardness in the HAZ which results from the inherent low alloy, high carbon equivalent nature of AISI 4140, especially when combined with fast cooling [2, 3]. This is a factor contributing to the susceptibility of high carbon equivalent steel hydrogen-assisted cracking [4], often referred to as cold cracking in relation to welding [5, 1]. Both of these key features have a negative effect on strength [1].

There are a number of strategies that can be employed to avoid these problems. When joining using fusion welding technologies the joint preparation (removal of moisture, dirt, oxides and rust) is vitally important to assure weld quality [2, 6]. When joining high carbon equivalent steel, only filler materials with a guaranteed low hydrogen content [2] and low hydrogen arcs should be used, in order to reduce the likelihood of hydrogen-assisted cracking [6]. Furthermore it is generally recognised that pre-heating and slow cooling of the part avoids the formation of hard microstructures such as martensite and bainite in the weld and HAZ [3, 5, 6]. This can also enable the release of residual stress. Although these strategies mitigate the issues there is a consequential associated time and cost penalty per weld.

Much arc welding is performed manually and therefore weld quality is largely dependent upon the skill of the welder and the environment they are working in. For these reasons Flash Butt Welding (FBW) is considered an option for the fabrication of drill pipe. In contrast to manual arc welding processes FBW offers a fast, automated solution independent of consumables or shielding gas. These advantages led to FBW being the early technology of choice when joining drill pipes.

However, the development of Rotary Friction Welding (RFW) rapidly changed the market. RFW offers the same advantages as FBW outlined above [7, 8], and in addition offers:

- Higher production rate [7, 9]
- Reduced labour demands [7]
- Reduced energy requirement [9]

These factors have contributed to making RFW the primary method of choice of joining drill pipes in the oil and natural gas industry [8, 10]. So much so that the use of RFW is the specified joining method in order to meet the requirements of current industry standards, e.g,API 5DP and BS EN IS ISO 11961. Friction welding produces joints of the highest integrity [8] that are recognised for their excellent mechanical properties [9]. Directional drilling requires a metallurgical bond strong enough to resist the high torque and highly loaded rotary tension. Friction welds have proven capability to withstand very high combined torsional, bending and impact loading [9].

The rapid, solid state<sup>†</sup> technology avoids defects caused by melting and solidification commonly resulting from fusion welding such as melting and solidification. Instead, instead resulting in a fine grained microstructure at the weld interface and a narrow heat affected zone [9]. Consequently, mechanical properties including rotating bend fatigue have been shown to be excellent [9] and in some cases as with bend testing the weld strength has been shown to be equal or superior to that of the parent material [10]. Furthermore, the lower peak temperatures of the process reduce intermetallic formation, allowing for a range of dissimilar materials to be joined.

Rotary Friction Welding specifically offers further advantages for manufacturing; as noted above the process is easily automated [9], and this automation can include supplementary processes such as post weld machining operations and heat treatment. As such the process is highly repeatable, efficient and economical [8]. When compared to arc welding RFW does not require pre-heating, a protective arc or any consumables [9] and as such doesn't encounter the same complications with hydrogen-assisted cracking. Crucially the RFW process is a simple and clean operation, which is significantly faster than its arc welding and resistance welding counterparts. These factors have all contributed to selected friction welding as the preferred joining method for drill pipes and other safety and performance critical applications [8].

## **1.2 Rotary Friction Welding**

RFW is a solid-state welding technique where two parts, in this case the pipe and the tool joint, are forged together using mechanical motion and heat generated by friction. One part is rotated while the other remains stationary and an axial force is applied between the two parts, as in Figure 1.

---

<sup>†</sup> Solid state welding is a group of processes that form joints in materials below the melting point without the need for welding consumables, filler metals etc

**Document:** D3.6 Impact of welding on coating integrity

**Version:** 1.0

**Date:** 23 November 2021

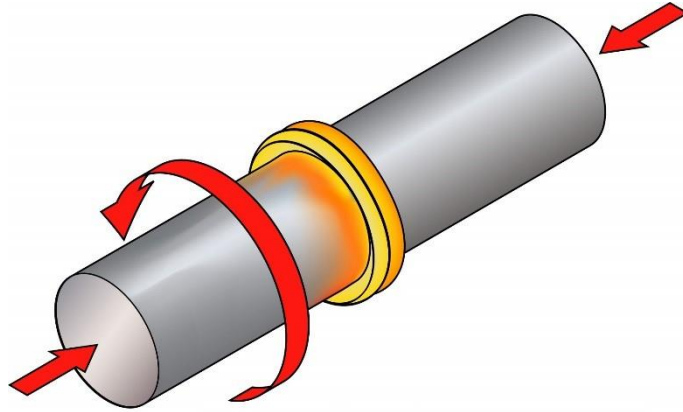


Figure 1: Schematic of rotary friction welding process

## 2. EXPERIMENTAL DETAILS

### 2.1 Rotary Friction Welding

#### 2.1.1 Materials

In this project welds will be produced from dissimilar materials steel alloys AISI 410 and N80. The accepted chemical compositions of the two alloys is shown in Table 1.

Material was procured with the following dimensions:

- N80 Tubes: 89mm outer diameter, 6.3mm wall thickness.
- AISI 4140 round bar: 90mm diameter.

Part lengths are measured prior to welding trials as shown in the following section.

Table 1 Material Composition

	AISI 4140	N80
Element	Content	
Carbon, C	0.380 - 0.430 %	
Chromium, Cr	0.80 - 1.10 %	
Iron, Fe	Balance	Balance
Manganese, Mn	0.75 - 1.0 %	
Molybdenum, Mo	0.15 - 0.25 %	
Phosphorous, P	≤ 0.035 %	≤ 0.030 %
Silicon, Si	0.15 - 0.30 %	
Sulfur, S	≤ 0.040 %	≤ 0.030 %

#### 2.1.2 Welding Equipment

A rotary friction welding (RFW) machine located at TWI Ltd Cambridge was used to carry out welding trials in this project. The machine selection was based on the size of the contact surface area for welding and the desired rotation speed. The work was conducted on large continuous drive rotary friction welding machine identified as FW3 (Figure 2). This machine was manufactured by TWI Ltd, and has the following specification:

Transmission power	75kW
Maximum welding force	1000kN
Maximum continuous rotation speed	1000rev/min
Guideline work piece diameter	30-100mm diameter solid bars in steel



Figure 2 Photograph of FW3

This machine is equipped with sensors to monitor rotation speed, axial displacement (burn-off) and welding pressure. These signals are recorded against time using a PC based package.

### 2.1.3 Part Preparation

Prior to welding, coupons are machined from received material. N80 tube was provided by Geolorn, the standard pipe dimensions were an outer diameter of 89mm, and inner diameter of 76.4mm and a length of 100mm. Based on final tool joint part geometries outlined by Geo-drill partners in WP5, representative AISI 4140 weld coupons were designed, the design is included in Figure 3. AISI4140 bar was purchased in 70mm outer diameter bar form, then machined to the dimensions indicated in Figure 2. Prior to welding, the welding interface of the coupons are faced to remove up to 0.5mm of material and leave a flat surface and improved surface finish. Once faced, coupons are cleaned and their length is measured immediately before welding, the length measurements are included in Table 2.

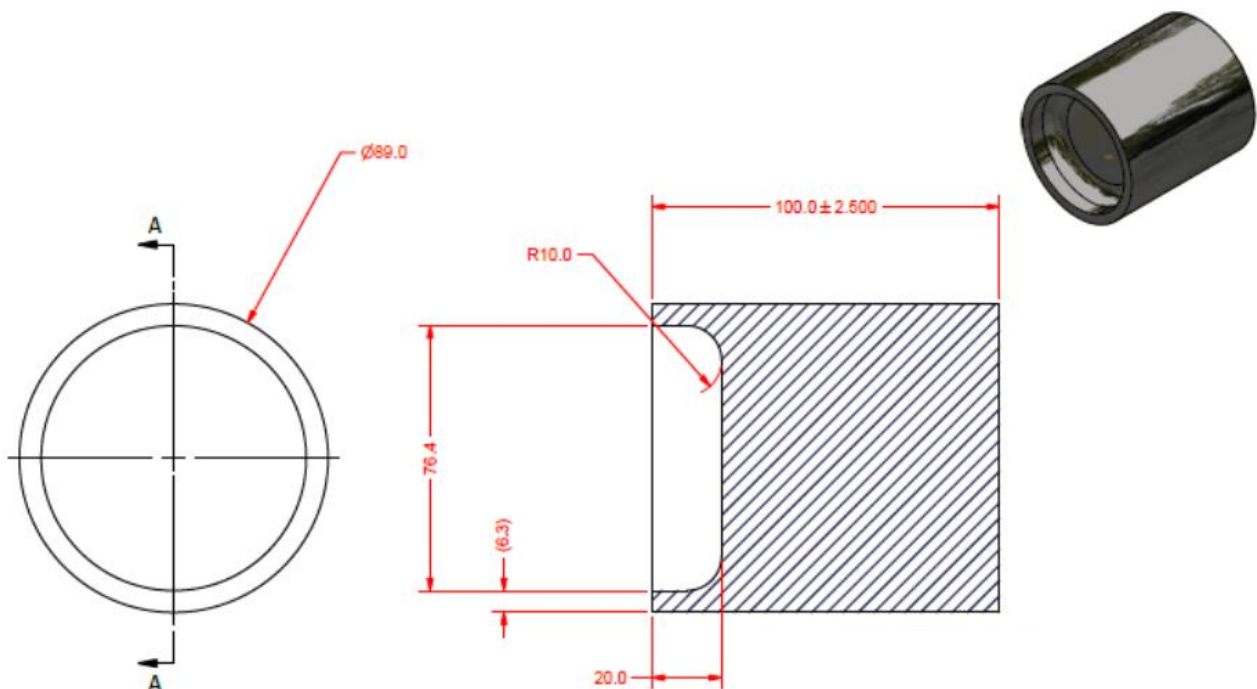


Figure 3 AISI 4140 coupon design

Table 2 Measured Part Lengths

Weld Number	Static part Length	Static Part Material	Rotating part length	Rotating Part Material
33004/3-w1	100.64	AISI 4140	99.25	N80 Tube
33004/3-w2	100.14	AISI 4140	99.6	N80 Tube
33004/3-w3	100.35	AISI 4140	99.11	N80 Tube
33004/3-w4	100.63	AISI 4140	99.43	N80 Tube
33004/3-w5	100.89	AISI 4140	98.38	N80 Tube
33004/3-w6	101.03	AISI 4140	98.91	N80 Tube
33004/3-w7	101.4	AISI 4140	98.68	N80 Tube
33004/3-w8	100.86	AISI 4140	98.59	N80 Tube
33004/3-w9	100.93	AISI 4140	99.06	N80 Tube
33004/3-w10	100.38	AISI 4140	98.89	N80 Tube
33004/3-w11	100.72	AISI 4140	99.46	N80 Tube
33004/3-w12	100.25	AISI 4140	98.28	N80 Tube
33004/3-w13	100.22	AISI 4140	99.59	N80 Tube
33004/3-w14	100.43	AISI 4140	98.42	N80 Tube
33004/3-w15	100.97	AISI 4140	99.39	N80 Tube
33004/3-w16	100.25	AISI 4140	99.77	N80 Tube
33004/3-w17	100.91	AISI 4140	97.93	N80 Tube
33004/3-w18	100.69	AISI 4140	99.08	N80 Tube
33004/3-w19	100.14	AISI 4140	98.54	N80 Tube
33004/3-W20	100.51	AISI 4140	98.57	N80 Tube
33004/3-w21	101.08	AISI 4140	98.14	N80 Tube
33004/3-w22	99.98	AISI 4140	98.24	N80 Tube

2.1.4 Welding Trials

The parameter ranges used for the RFW studies were based on experience developed at TWI from research into comparable conditions (material type and gauges). The values explored for the RFW trials are shown in Table 3. Figure 4 provides greater detail of the welding set up, the welding coupons can be seen held in collets prior to welding.

Table 3 RFW trial parameter investigation range

RFW Parameter	Value
Rotational speed (RPM)	600-800
Touch down force (kN)	33
Friction force (kN)	120-240
Forging force (kN)	270-385
Stationary component	AISI 4140
Rotating component	N80

Pre-set burn-off (mm)	3-9
-----------------------	-----

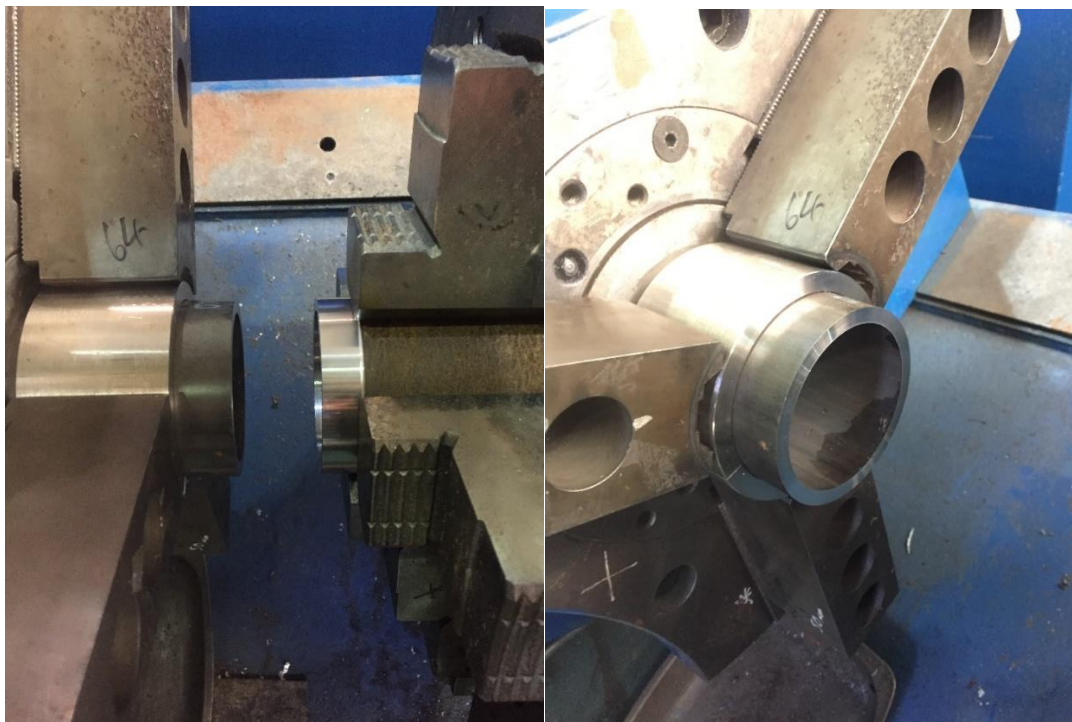


Figure 4 Photographs of welding set up.

### 2.1.5 Metallurgical analysis

The soundness of a weld is typically assessed by a combination of visual and metallographic examination and mechanical testing. While a trained eye can identify the tell-tale signs of underlying problems, the user perceived aesthetic ‘quality’ of a weld is very subjective. The very nature of the friction welding process results in hot shears and subsequent re-crystallisation of both plate and plug material to give a very fine grained structure. Welds are generally considered to be acceptable if the metallographic examination shows that such modifications are local to the welded interface and fails to reveal any flaws or unwelded regions.

As part of the current project sections will be cut from completed welds, then mounted and polished. Macro images will be taken of the weld interface on an optical microscope, these will be used to assess weld quality, in terms of the presence of defects at the weld interface and/or corner flaws. Sections will also be assessed using a hardness traverses to measure the hardness variation in different regions of the weld and surrounding material.

### 2.1.6 Tensile testing

A simple cross weld tensile test piece will be cut from every weld made and tested to provide a comparative strength value. Samples will be machined to a known diameter and length, with the weld positioned half way along this length. Tensile loading will be applied using a Denison tensile test machine and the load and position of fracture was recorded. Three tests will be undertaken per weld parameter set at ambient temperature.

### 2.1.7 Design of Experiments

A full factorial DOE matrix is completed using welding parameters outlined in Table 3. Measurements of peak hardness and ultimate tensile strength values will be used as response values to optimize parameter selection. Regression analysis and optimisation is achieved utilising SigmaZone DOE PRO software.

## 2.2 Coating deposition

### 2.2.1 Materials

Two different types of coatings were sprayed on prepared weld sections, one is WC coating and the other is self-fluxing coating. Detailed information of both powders is listed in Table 4.

Table 4 Powders used for HVOF coatings on welds.

TWI ID	Powder	Chemistry	Size, $\mu\text{m}$	Supplier	Max temp, $^{\circ}\text{C}$
4278	Woka 3652 FC	WC10Co4Cr	-45+15, sub	Oerlikon metco	500
4279	1660-02	NiCrFeSiB	-50+20	Hoganas	820

Weld sections were prepared using parameters defined from DoE matrix, as shown in Figure 5. Prior to applying coatings, the weld surface of AISI 4140 bar and N80 pipe was grit-blasted to remove surface contaminants and to create a rough surface for better adhesion. Surface preparation parameters are described below:

- Blast media: alumina;
- Mesh size:60;
- Running air pressure:60 psi;
- Stand-off distance: 80mm;
- Abrasive nozzle:  $\varnothing=8\text{mm}$  ID.

The roughened surface was then cleaned using compressed air and alcohol. Coating deposition was carried out immediately on the freshly prepared surface.

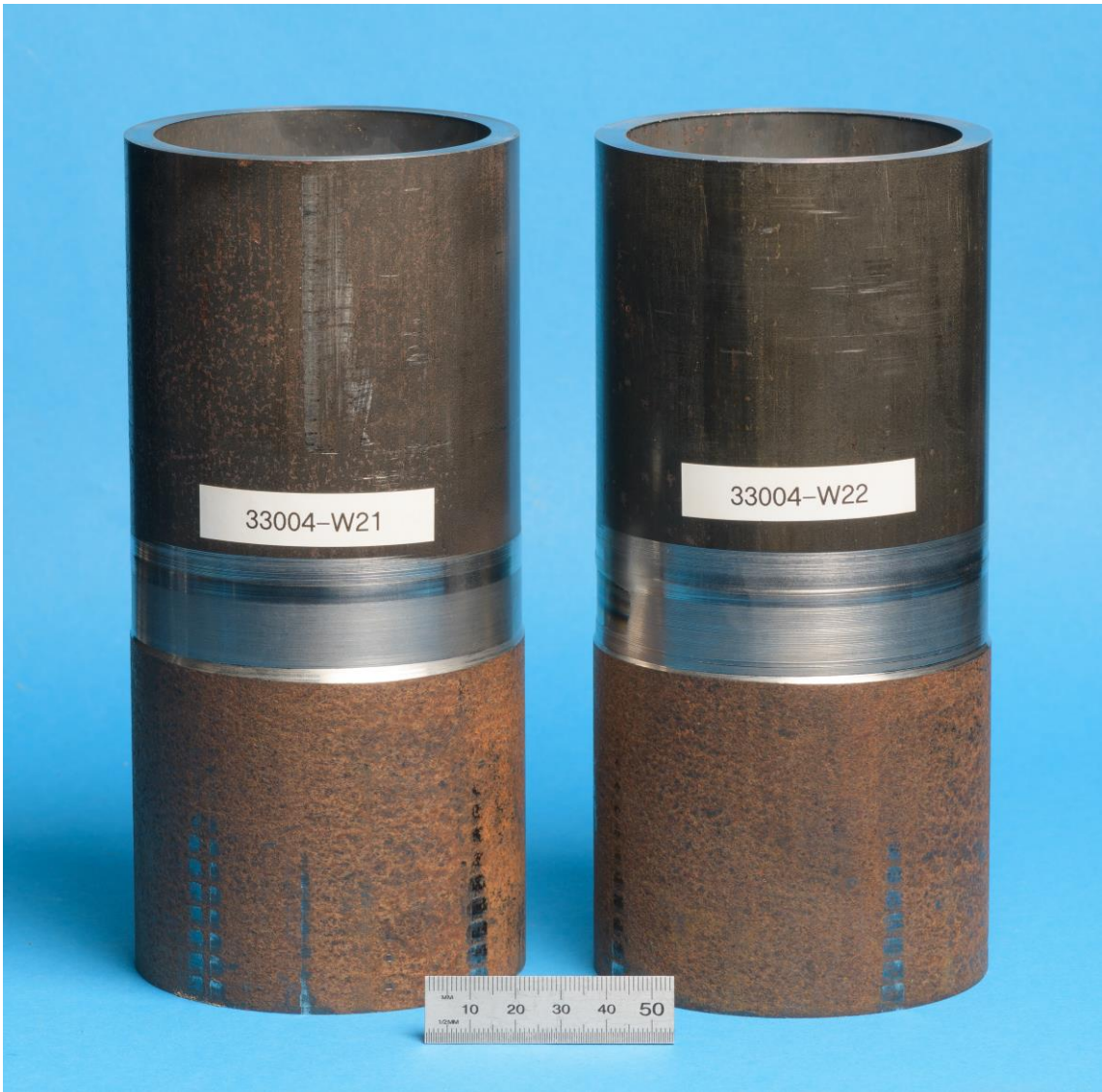


Figure 5 Two welds used for coating deposition.

**2.2.2 HVOF spray set-up**

The Tafa JP5000 HVOF system at TWI, manufactured by Praxair Surface Technologies, was used for coating deposition in this work (Figure 6). Powder was fed radially into the gun through a two-way powder feeder. Liquid kerosene and oxygen were supplied to the spraying gun using a Tafa 5120 control console. Powder was fed into the gun using a Tafa model 550 hopper, and cooling water was applied and controlled using a PTC model TAE301 heat exchanger unit. Best spray parameters defined in D2.4 report were used for each powder for coating deposition. Details are presented in Table 5.

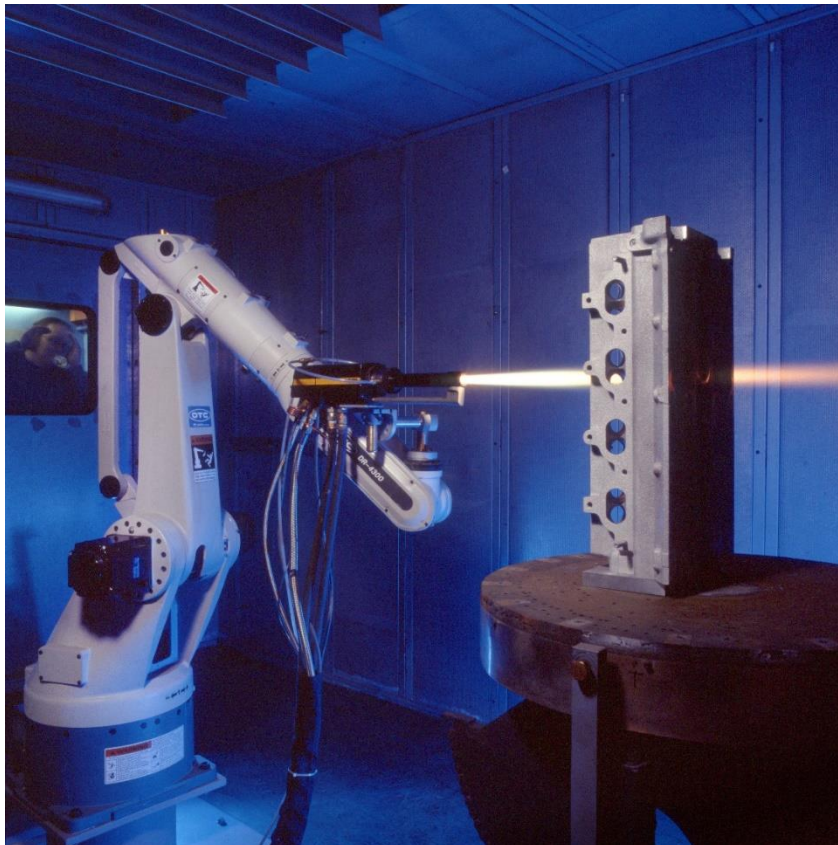


Figure 6 Tafa JP5000 HVOF system (Kerosene) at TWI, Cambridge.

Table 5 Spray parameters for WC-CoCr and self-fluxing coatings.

Parameters	WC-CoCr coating	Self-fluxing coating	Ni-based
ID	36WC	36Flux	
Powder	Woka 3652 FC	1660-02	
Weld substrate	W21	W22	
ID used in WP2	232WC	234Flux	
Spray angle, °	90	90	
Powder carrier gas	Argon	Argon	
Gun traverse speed, mm/s	900	900	
Increment, mm	5	5	
Specimen cooling	Air	Air	
Nozzle	6 inch	4 inch	
Powder feeder	Two-way	Two-way	
Powder feed rate, rpm	350	150	

Carrier gas flow rate, scfh	23	26
Spray distance, mm	350	380
Oxygen flow, SLPM	920	930
Kerosene flow, SLPM	0.400	0.385

### 2.3 Coating Characterisation

Coatings deposited on welds were assessed in terms of coating microstructure and mechanical property using a combination of the following methods.

#### 2.3.1 Microstructure characterisation

To analyse coating’s microstructure, the samples were cross-sectioned and then cold-mounted in epoxy. Both samples were ground with silicon carbide papers with various grits then polished with diamond (3 and 1 µm) and colloidal silica (0.02 µm) suspensions.

Optical microscopy was used to do preliminary check of the cross-sectioned samples. Then scanning electron microscopy (SEM) equipped with energy dispersive X-ray spectroscopy (EDX) was used to further study microstructure of samples. Images at different magnifications were taken, mainly in backscattered mode for higher contrast between pores, oxide areas and metal matrix. EDX spectroscopy was employed while imaging on SEM to obtain the elemental compositions at different areas of the sample cross-sections.

#### 2.3.2 Scratch test

RINA-CSM has supported TWI to carry out scratch test to study how the coating adhere to the heat-affected zone (weld area) compared with parent steels. It was conducted on the polished cross-section surface of the sprayed coatings. A constant load was applied from substrate towards coating. Three areas were checked for each sample, including N80 side, 4140 side, and weld area. An image of the scratched area was taken after testing in order to determine failure mode. Failure was determined by checking location of cracks generated. Adhesion failure is determined by failure happened at coating/substrate interface, and cohesive is failure in the coating. Detailed information of test condition is listed in Table 6.

Table 6 Scratch testing parameters used in this report.

Parameter	Value
Load (N)	30
Speed (mm/min)	0.7
Indenter	Rockwell Diamond (100 µm radius)

### 3. RESULTS AND DISCUSSION

#### 3.1 Welding Trials

A design of experiments (DOE) matrix was prepared to assess parameter modification on weld quality. Four parameters were varied within the matrix:

- Rotation speed
- Friction force
- Forge force
- Burn off distance

The matrix can be found in Table 7, where parameters are related to the weld number. Photographs of the completed welds can be found in Appendix A. Visually all welds were satisfactory, no external defects were identified.

Table 7 Input parameters employed in welding trials

Weld Number	Rotation Speed (RPM)	LTD Force (kN)	LTD Time (s)	Friction Force (kN)	Forge Force (kN)	Burn off distance (mm)
33004/3-w1	600	33	2	198	385	3
33004/3-w2	600	33	2	198	385	6
33004/3-w3	600	33	2	198	385	9
33004/3-w4	600	33	2	120	270	3
33004/3-w5	600	33	2	120	270	6
33004/3-w6	600	33	2	120	270	9
33004/3-w7	600	33	2	240	385	6
33004/3-w8	600	33	2	198	270	6
33004/3-w9	600	33	2	120	385	6
33004/3-w10	600	33	2	120	385	3
33004/3-w11	600	33	2	198	270	3
33004/3-w12	800	33	2	120	385	3
33004/3-w13	800	33	2	198	270	3
33004/3-w14	800	33	2	120	385	6
33004/3-w15	800	33	2	198	270	6
33004/3-w16	800	33	2	120	270	3
33004/3-w17	800	33	2	120	270	6
33004/3-w18	800	33	2	198	385	3
33004/3-w19	800	33	2	198	385	6
33004/3-W20	800	33	2	120	270	6

### 3.1.1 Cross Weld Tensile Testing

Each weld was subject to tensile testing, ultimate tensile strength measurements for each weld can be found in Figure 7. Photographs of the failed tensile samples can be found in Appendix B. N80 parent material displays a UTS of approximately 689N/mm<sup>2</sup>. The majority of cross weld tensile tests result in a UTS equal to or greater than that of the baseline parent material, these samples are observed to show ductile failure in the parent material. Some show a reduction in tensile strength when failing in the parent material, for example W10, W12 and W13, and these failures are observed to be less ductile in nature.

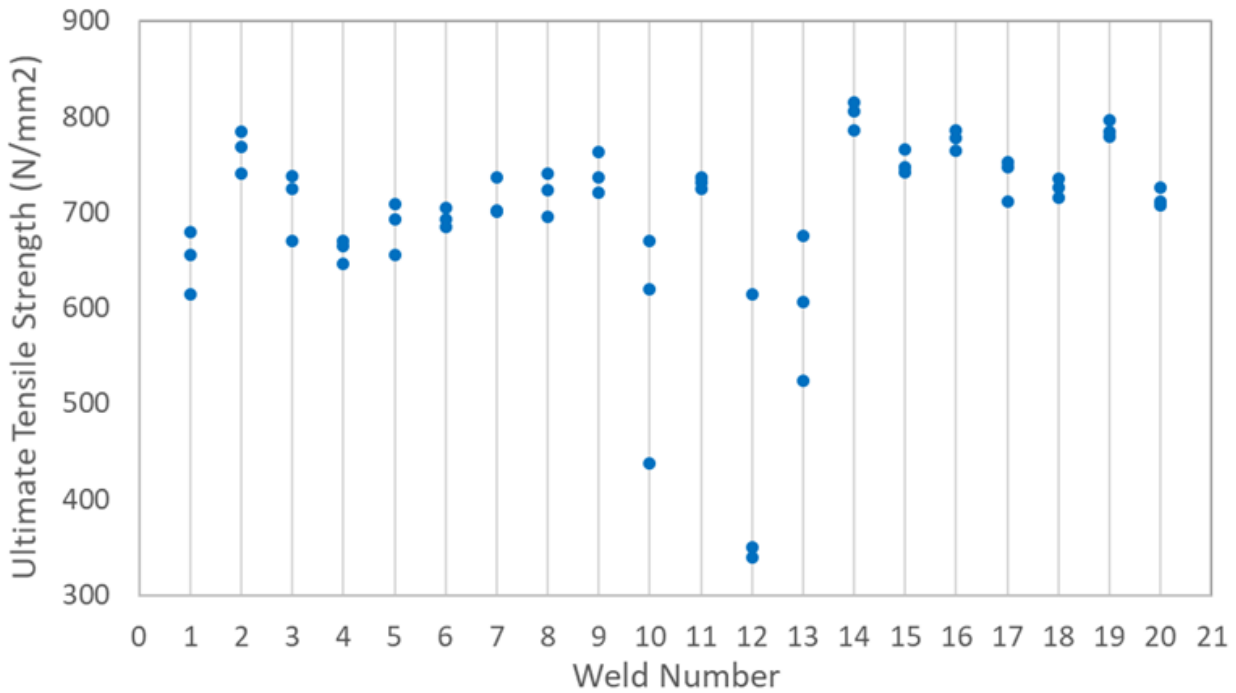


Figure 7 Ultimate tensile strength measurements for each weld

### 3.1.2 Microstructural assessment

Macro graphs of the weld interface were taken for each weld, examples can be found in Appendix C. Assessment of the micro-graphs revealed no presence of defects at the weld interface and/or corner flaws, furthermore the welds display uniformity across the weld interface.

Polished samples are used for hardness profiling, the resulting hardness profile in all joints displays a hardness peak at the interface, and example of this can be observed in Figure 8. Hardness at the weld interface is seen to increase up to three times the hardness of the parent material. It can be seen that the increase in hardness is associated with deformation within the microstructure close to the weld interface, this is highlighted by the change in visual appearance of material close to the weld interface in Figure 8 a. The peak hardness found in each hardness profile across the weld interface is detailed in Table 8, this information was used in the DoE matrix.

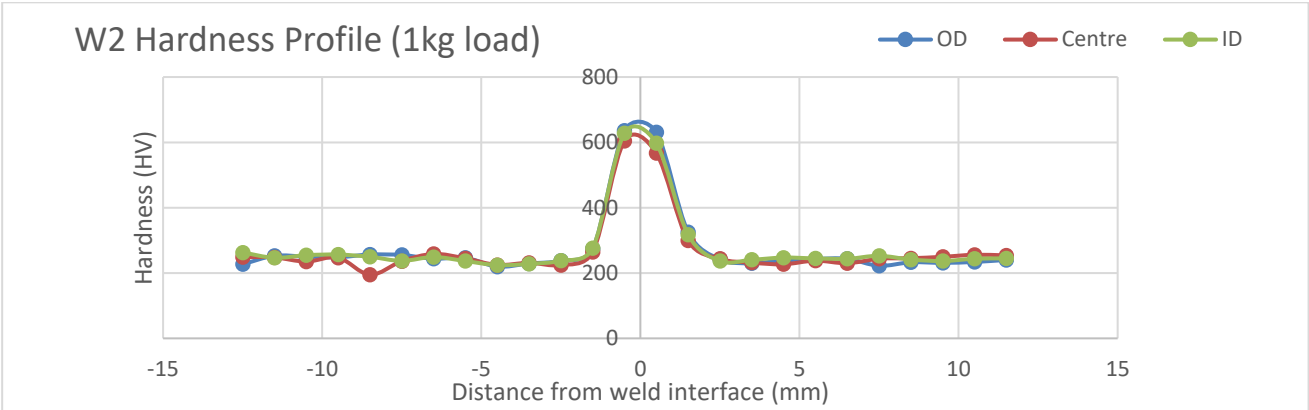
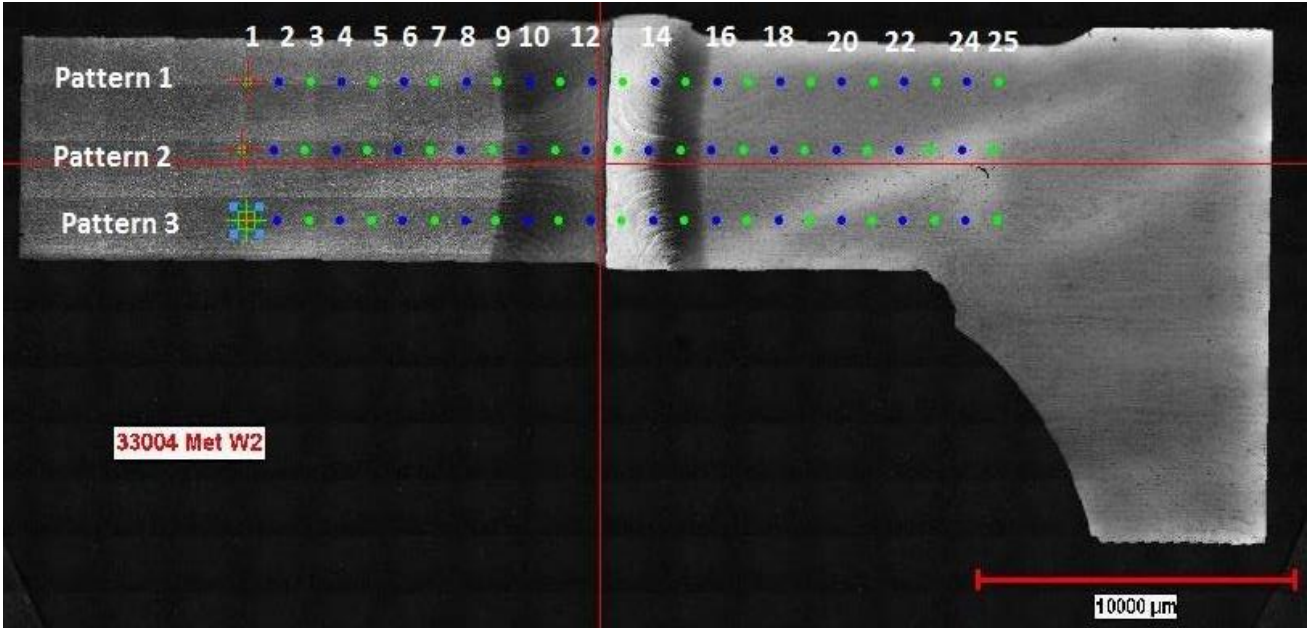


Figure 8 W2 a) Hardness indent locations b) Hardness profile across the weld interface at three locations outer diameter (OD), centre and inner diameter (ID)

Table 8 Peak hardness measurements at the weld interface at three locations outer diameter (OD), centre and inner diameter (ID)

Weld Number	Peak Hardness (HV)		
	OD	Centre	ID
33004/3-w4	619	607	619
33004/3-w5	633	614	619
33004/3-w10	631	607	621
33004/3-w9	631	611	623
33004/3-w11	633	688	631
33004/3-w8	683	688	685
33004/3-w1	688	651	628
33004/3-w2	636	604	628
33004/3-w16	614	631	631
33004/3-w17	626	619	619
33004/3-w12	619	628	616
33004/3-w14	646	651	631
33004/3-w13	616	628	633
33004/3-w15	653	638	653
33004/3-w18	638	641	628
33004/3-w19	675	669	638

### 3.1.3 Design of Experiments

Using the DOE software for multiple response optimisation aiming to minimise peak hardness, maximise ultimate tensile strength, revealed the following optimal input settings:

- Rotation speed: 800rpm
- Friction force: 120kN
- Forge force: 270kN
- Burn off distance: 3mm

These welding parameters were utilised to produce two further welds for coating trials. Table 9 shows the multiple response prediction when using the parameters outlined above.

Table 9 Multiple Response Prediction (Y-hat = the predicted response, S-hat = standard deviation)

	Y-hat	S-hat	99% Confidence Interval	
			Lower Bound	Upper Bound
Ultimate Tensile Strength	778.9988	11.6599	744.019	813.979
Peak Hardness	624.2083	8.3716	599.094	649.323

### 3.2 Coatings on welds

Two welds were coated with selected cermet and alloy coatings from WP2 using HVOF spraying. One is WC-CoCr coating (36WC) and another is self-fluxing coating (36Flux). Digital image of coated welds is shown in Figure 9. Both coatings present a uniform surface condition along the weld area and parent steel area.

To study microstructure of both coatings, further analyses were carried out (Figure 10 - Figure 15). Three areas were studied for each sample at higher magnifications using SEM, including N80 parent side, 4140 parent side, and weld area, as illustrated in Figure 11 and Figure 14.

- Results for 36WC coating indicate that the deposited WC-CoCr coating adhered well along the weld surface and the coating presents a uniform microstructure on three different areas (Figure 10, Figure 12). Cracking is observed on the coating top-surface but not in the coating. This probably occurs during the sample metallography preparation process due to the brittle nature of WC coating. This will work against extending the operating life of hammer parts. Therefore, special care should be taken if any post-treatment is needed for this coating when being applied on hammer prototypes.
- Results for 36Flux coating indicate that the deposited self-fluxing (NiCrFeSiB) coating also adhered well along the weld surface and has a uniform microstructure (Figure 13, Figure 15). Both coating thickness and porosity seem to be similar at the three different areas. No sign of cracking is seen from SEM images.

Scratch test was also carried out at the polished cross-section surface of both samples to study whether the coating adhere to the substrate as well at different areas as illustrated in Figure 11 and Figure 14.

- Scratch test results on 36WC sample show that failure was observed in the coating for N80 side and weld area (heat-affected area), indicating adhesion failure (Figure 16). While coating delamination is observed at coating-substrate interface for 4140 side, indicating cohesive failure.
- Scratch test on 36Flux sample shows similar results as 36WC (Figure 17). Cracking is observed in the coating on N80 side and weld area, indicating adhesion failure. Coating cracking is seen at the coating-substrate interface for 4140 side, indicating cohesive failure.

In summary, Rotary Friction Welding does not seem to have an impact on coating integrity. Both cermet and alloy HVOF sprayed coatings seem to behave similarly in the weld area (Heat affected zone) as compared with parent metals.

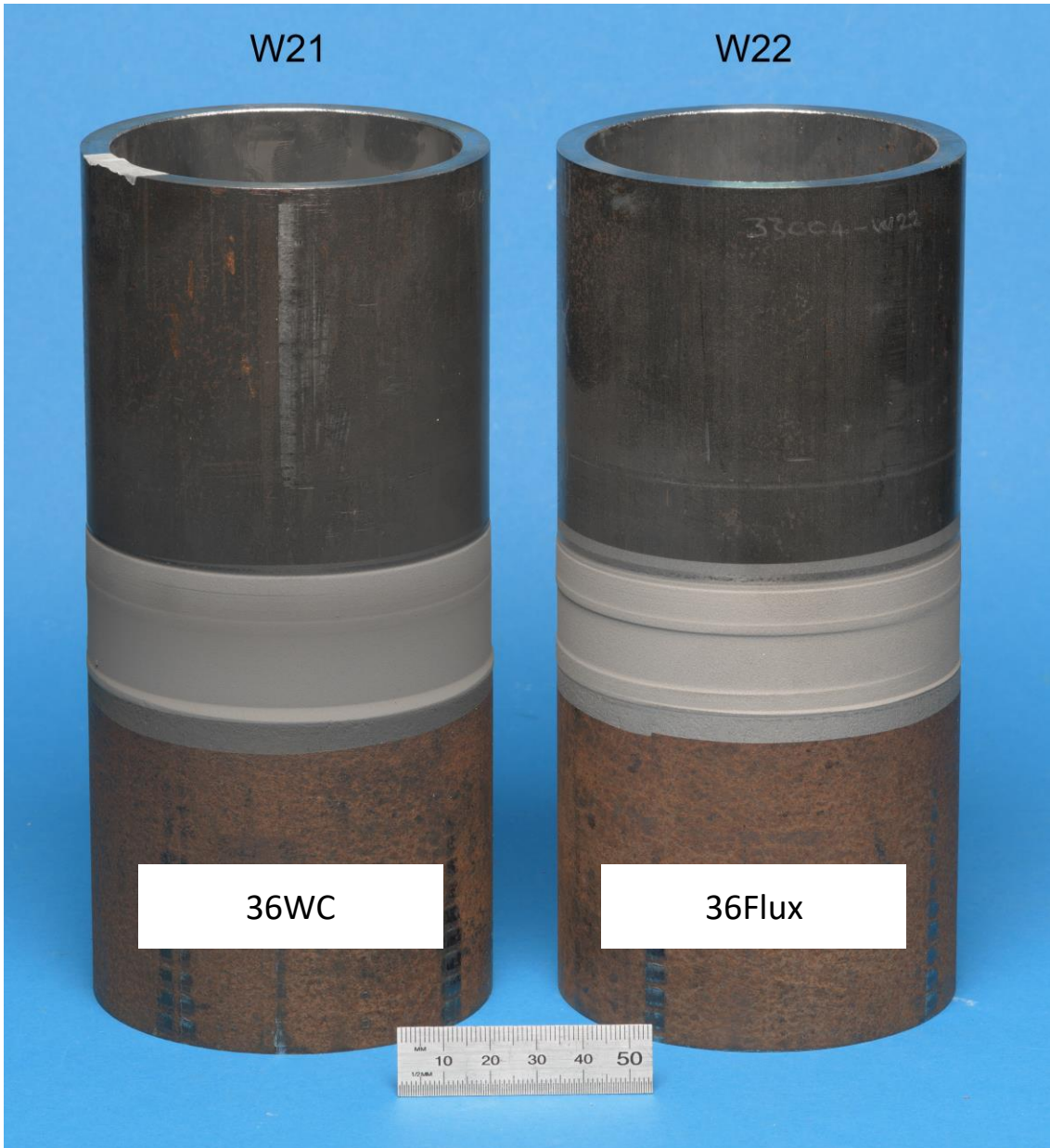


Figure 9 Coatings 232WC and 234Flux deposited on welds

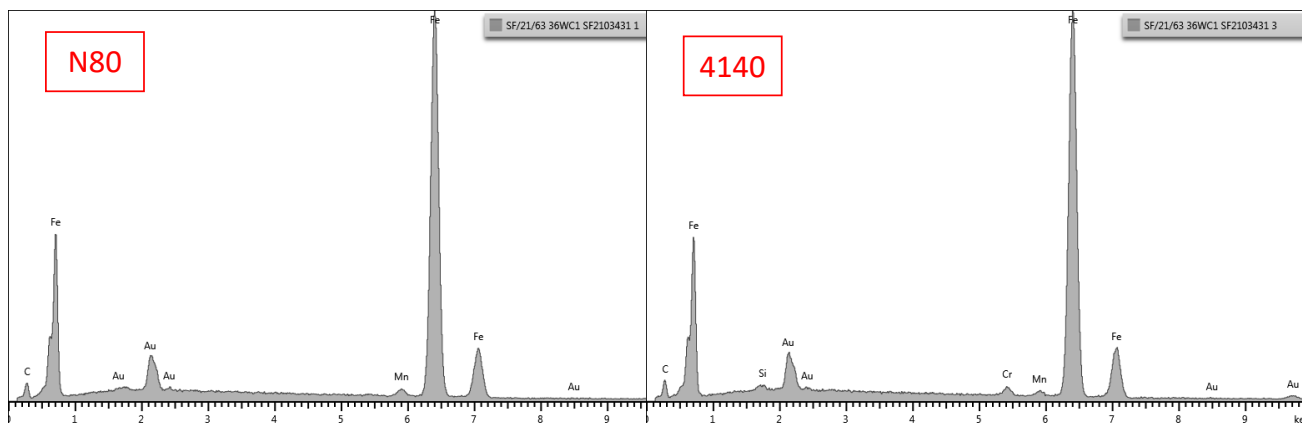
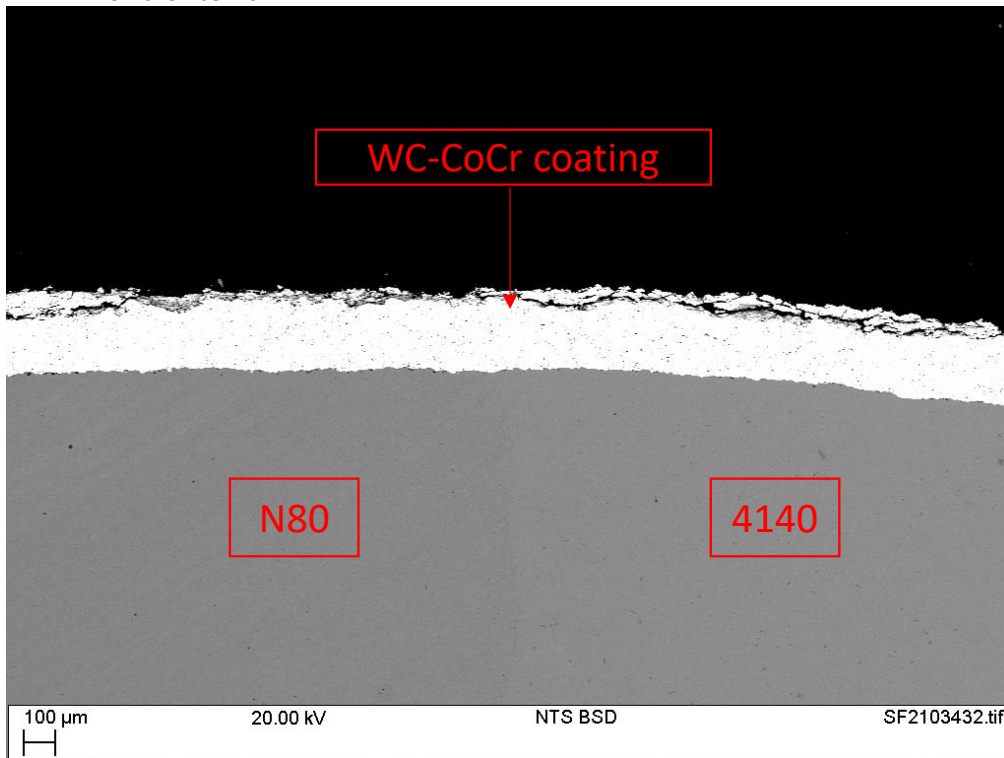


Figure 10 SEM and EDX analyse of sample 36WC at low magnification

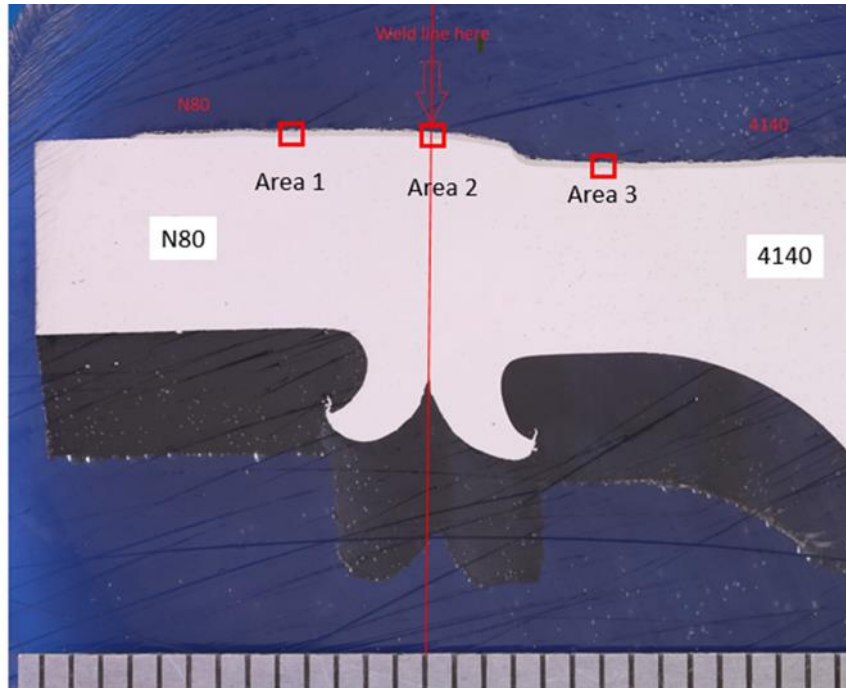


Figure 11 Optical microscopy images of polished cross-sectional surface of 36WC, illustrating areas of interest for SEM and EDX analyse.

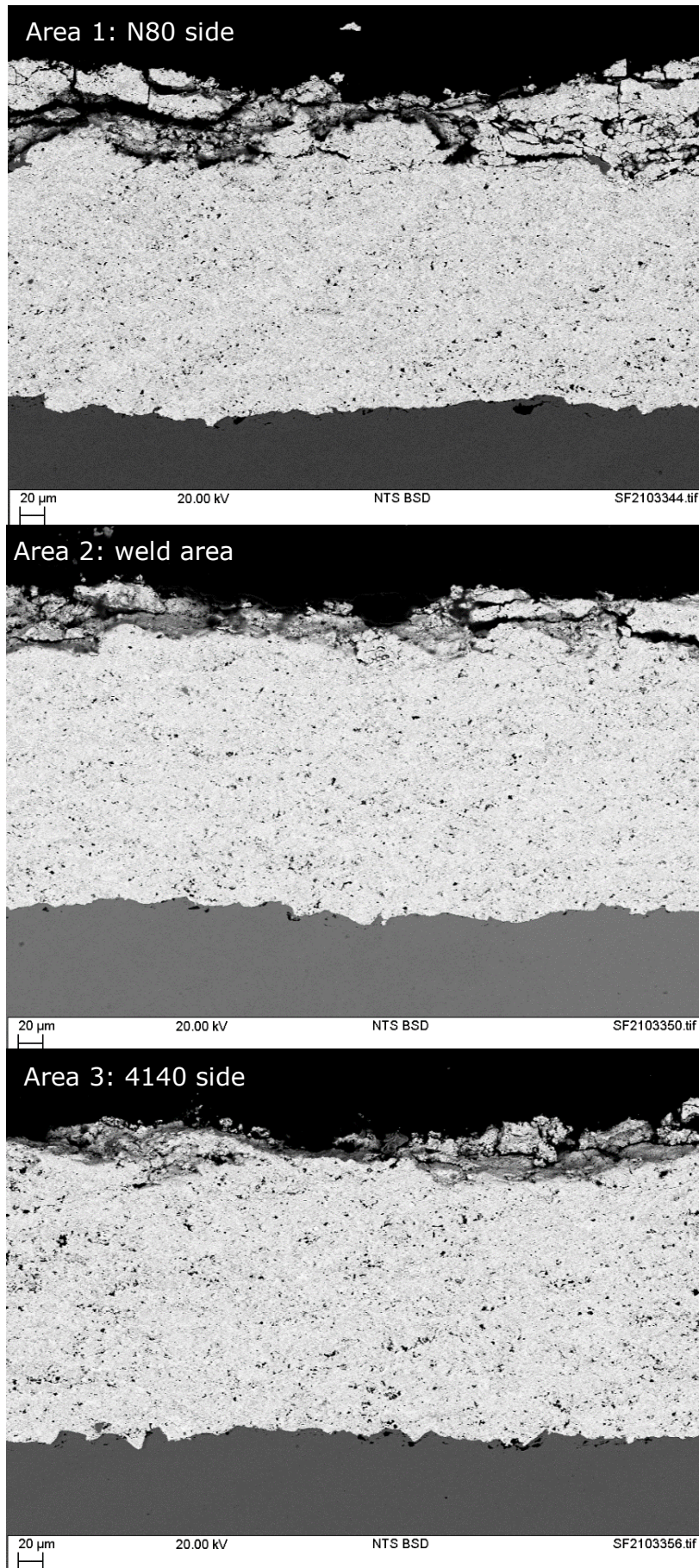


Figure 12 SEM analyse of sample 36WC at higher magnification



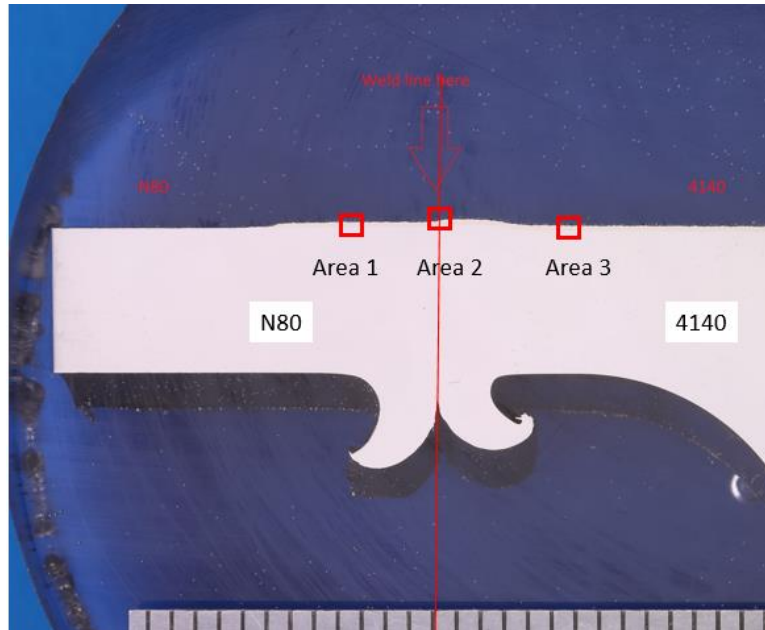


Figure 14 Optical microscopy images of polished cross-sectional surface of 36Flux, illustrating areas of interest for SEM and EDX analyse.

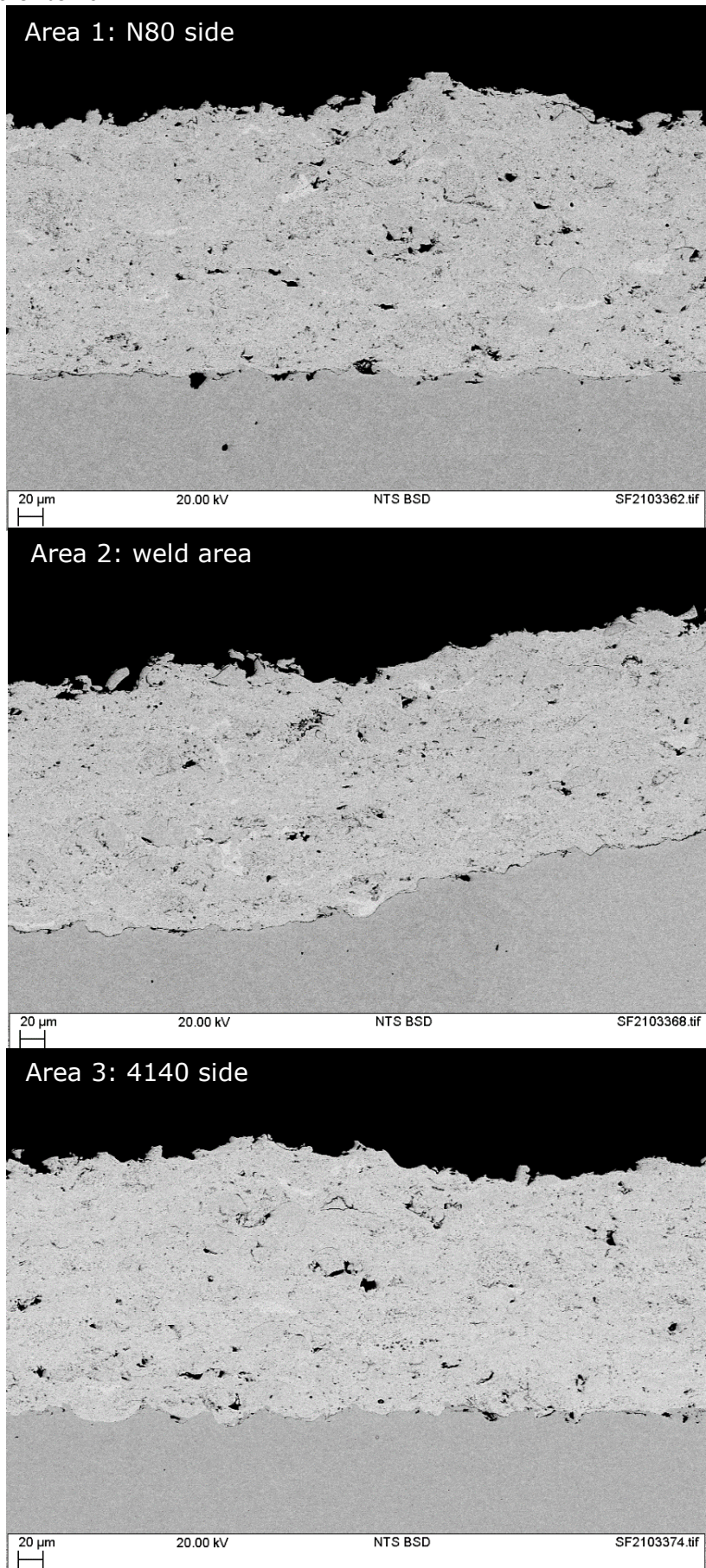


Figure 15 SEM analysis of sample 36Flux at higher magnification

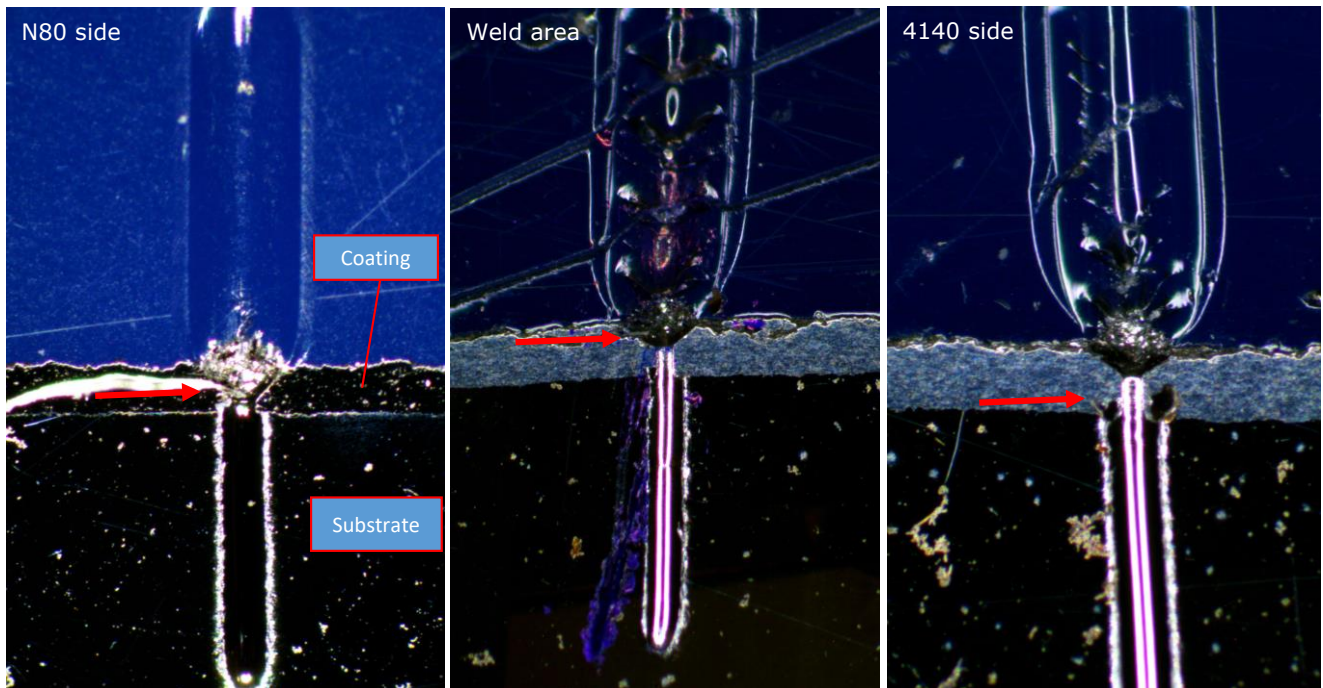


Figure 16 Images of scratch on polished cross-section surface of 36WC at three different areas

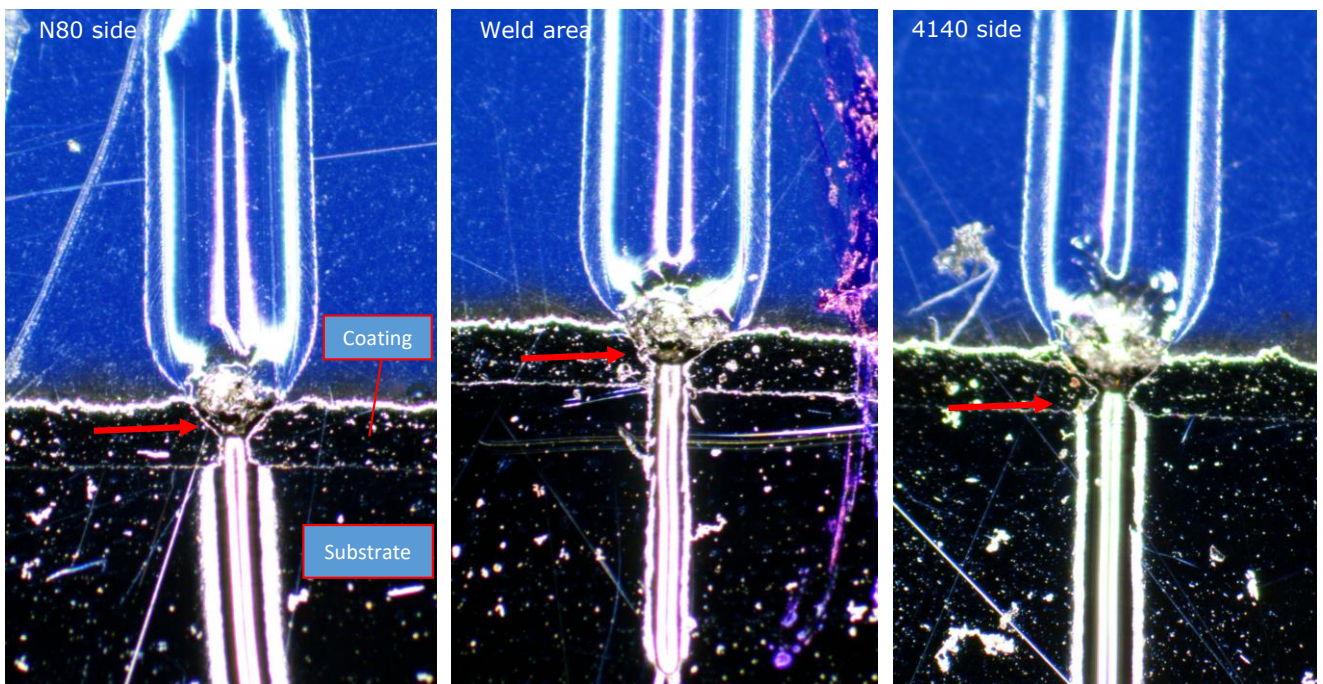


Figure 17 Images of scratch on polished cross-section surface of 36Flux at three different areas

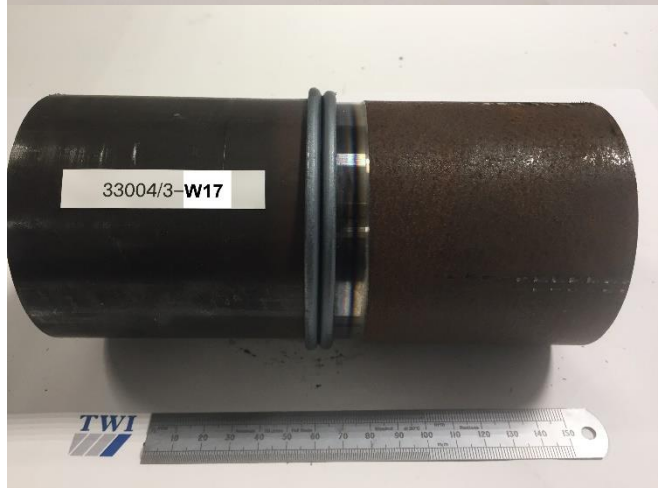
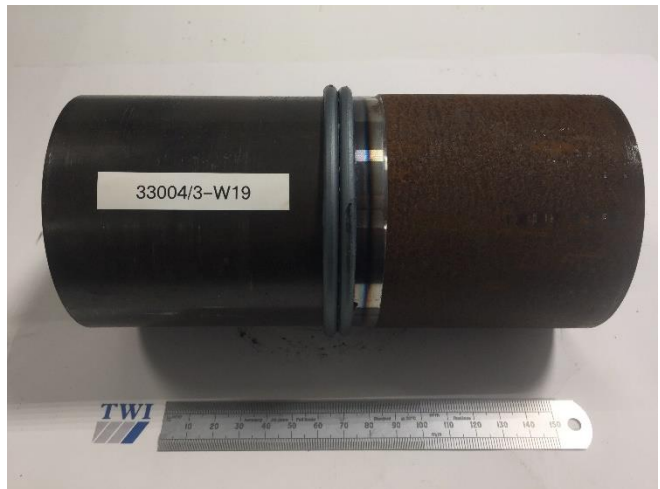
## 4. CONCLUSIONS

- Rotary friction welding has proved capable of creating high integrity, uniform, and defect free joints.
- The following optimal input settings were identified to minimise peak hardness and maximise ultimate tensile strength:
  - Rotation speed: 800rpm
  - Friction force: 120kN
  - Forge force: 270kN
  - Burn off distance: 3mm
- The rotary friction welding process is not seen to have an impact on the coating integrity. Both cermet and alloy HVOF sprayed coatings seem to behave similarly in the heat affected zone as compared with parent metals.

## REFERENCES

- [1] M. S. M.A. Wahap, "Corrosion and biaxial fatigue of welded structures," *J Materials Process Technology*, vol. 410, pp. 143-144, 2003.
- [2] K. Weman, "Welding processes handbook.," ProQuest Ebook Central , 2011.
- [3] N. Yurioka, "Physical metallurgy of steel weldability," *ISIJ International*, vol. 41, no. 6, pp. 566-570, 2001.
- [4] B. C, L. B and R. P, "Welding consumable optimisation for the welding of high and very high yield strength steels," *Competence*, no.5, pp. 15-24, 2010.
- [5] R. W. J. Messler, "A Practical Guide to Welding Solutions : Overcoming Technical and Material-Specific Issues," John Wiley & Sons, Incorporated, 2019.
- [6] I. B, "The challenge of welding heat treatable alloy steels.," *Welding Journal*, vol. 74, no. 2, pp. 43-48, 1995.
- [7] N. E. D, "Where industry uses friction welding. (part 2)," *Welding design and fabrication*, vol. 50, no. 8, pp. 74-76, 1977.
- [8] "Friction welding redefines design guidelines," *Welding and Metal Fabrication*, vol. 64, no. 9, pp. 21-22, 1996.
- [9] H. C. B, "Groundbreaking rules [friction welding drill pipe]," *Welding and Joining*, pp. 13-15, 1997.
- [10] S. P. M, T. Y. A, S. N. V and T. I. G, "Aspects of friction welding drill pipes," *Welding International*, vol. 4, no. 9, pp. 734-736, 1990.

APPENDIX A: Photographs of complete welds





Document: D3.6 Impact of welding on coating integrity

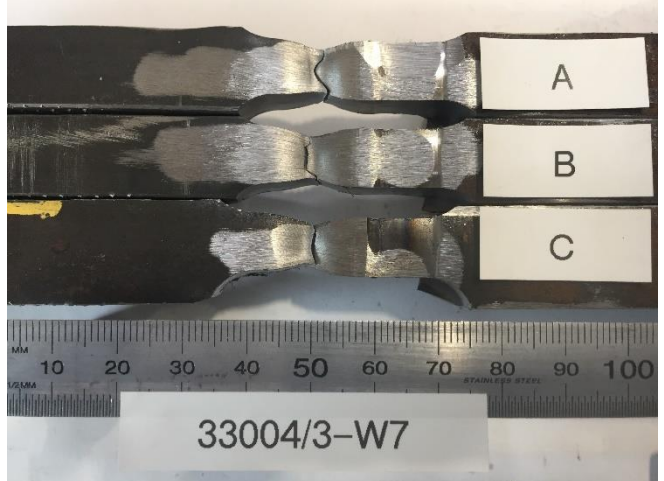
Version: 1.0

Date: 23 November 2021

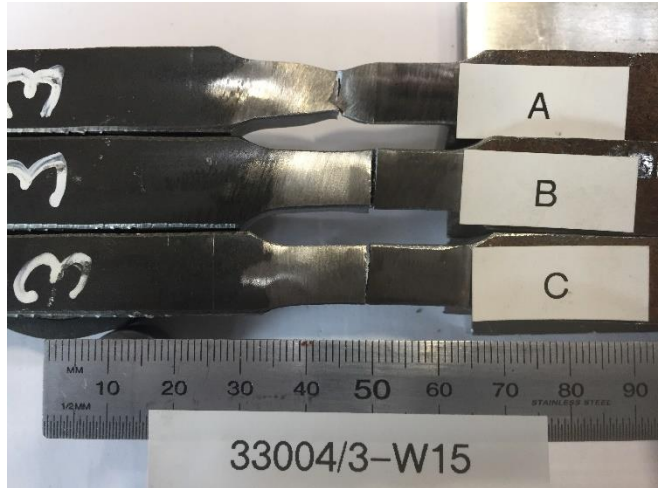




**APPENDIX B: Photographs of failed tensile samples**

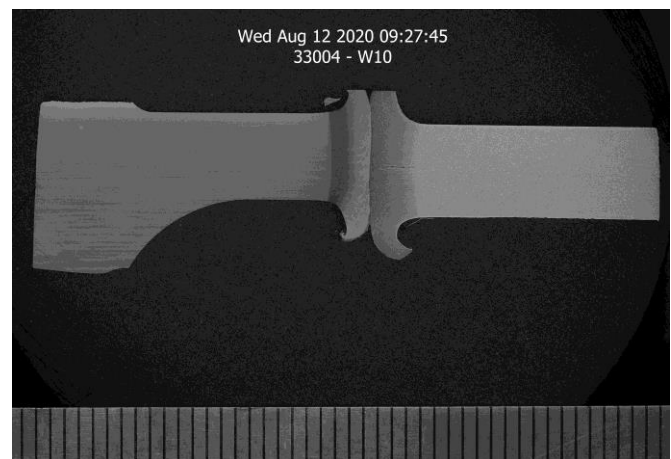
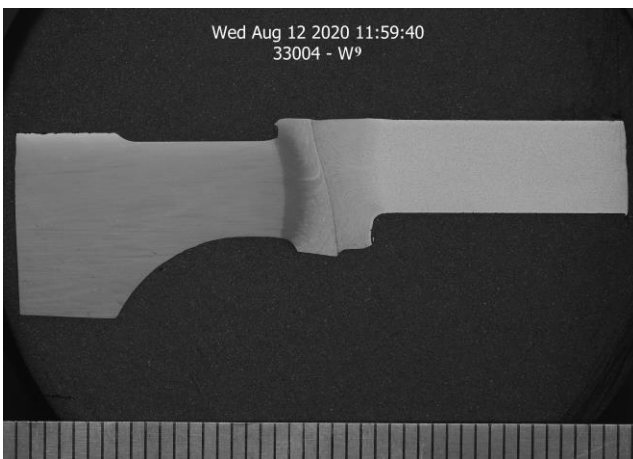
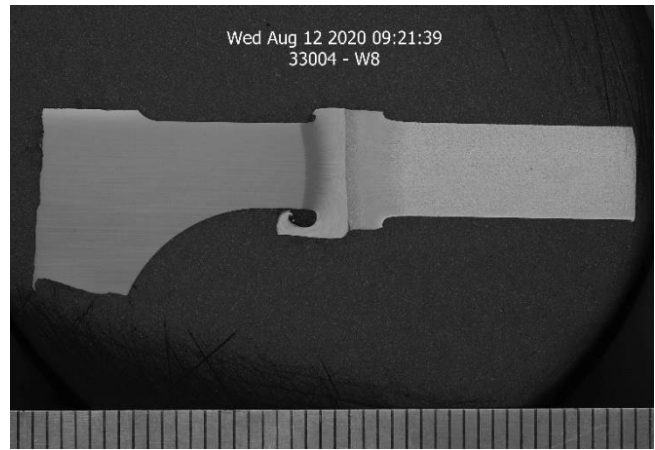
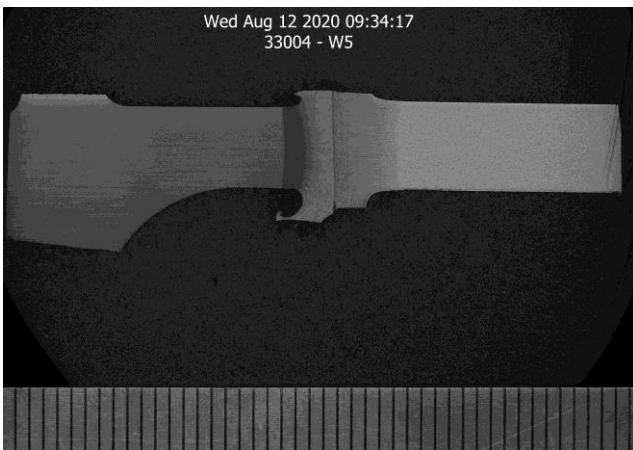
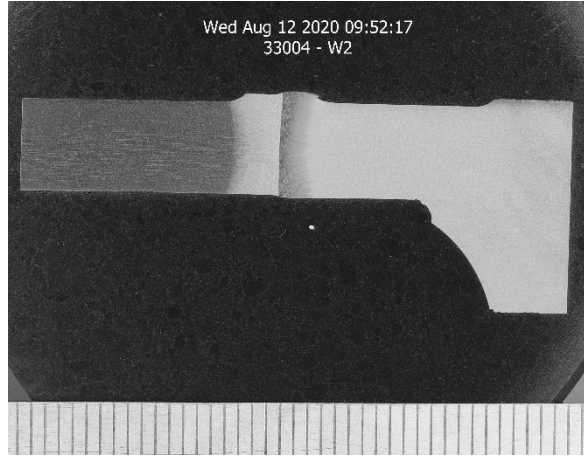
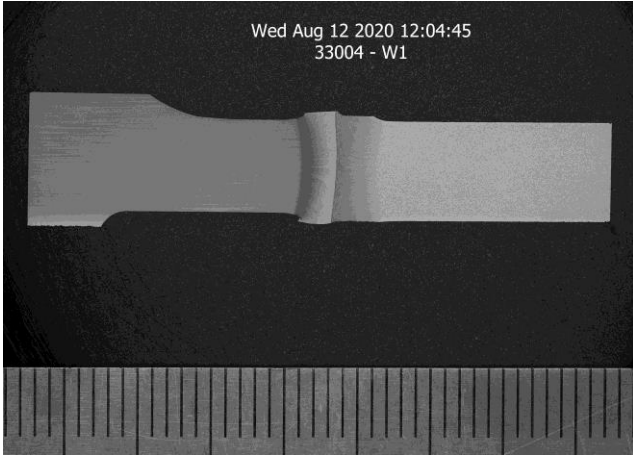








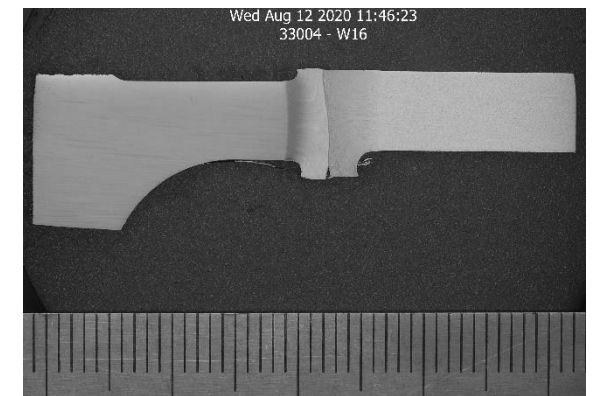
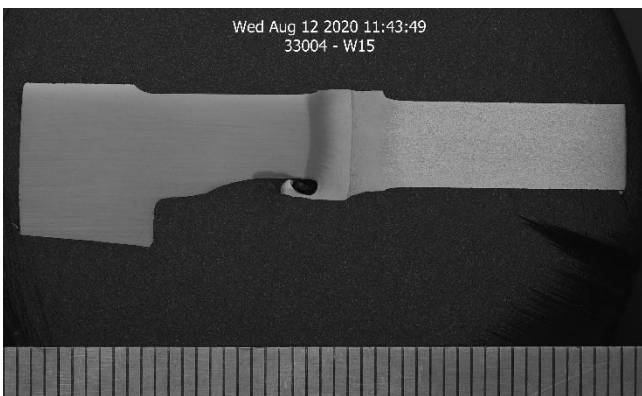
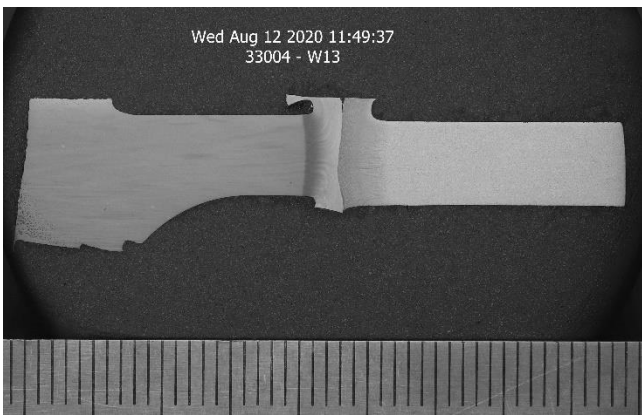
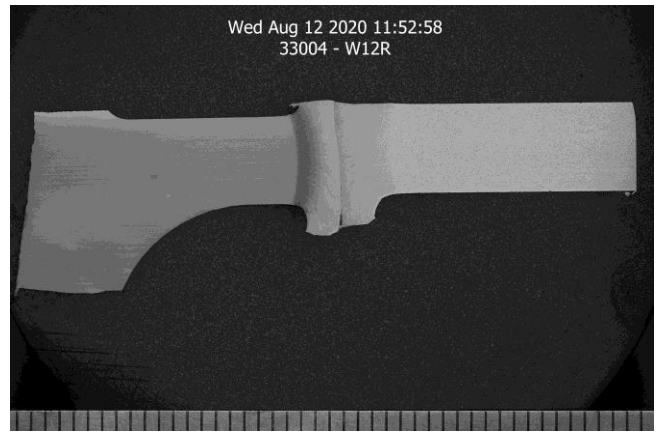
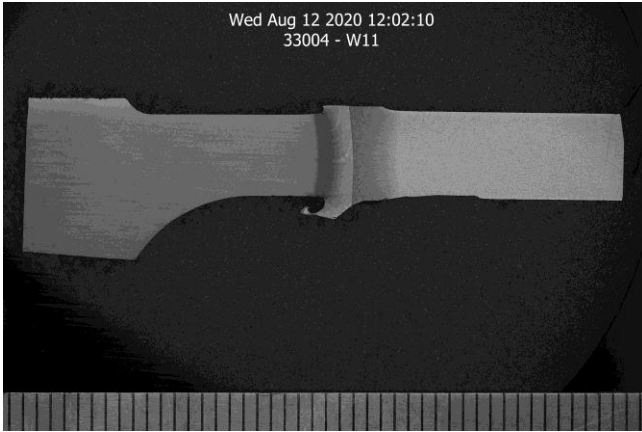
### Appendix C: Macro-images of the weld interface



Document: D3.6 Impact of welding on coating integrity

Version: 1.0

Date: 23 November 2021



**Document:** D3.6 Impact of welding on coating integrity

**Version:** 1.0

**Date:** 23 November 2021

